A new clinically-relevant rat model of letrozole-induced chronic nociceptive disorders

Aurore Collin, Julie Vein, Y. Wittrant, Bruno Pereira, Raalib Amode, Christelle Guillet, Damien Richard, Alain Eschalier, David Balayssac

A new clinically-relevant rat model of letrozole-induced chronic nociceptive disorders

Aurore Collin[1], Julie Vein[1], Yohann Wittrant[2], Bruno Pereira,[3] Raalib Amode[4], Christelle Guillet[5], Damien Richard[6], Alain Eschalier[1], David Balayssac[7*]

1. Université Clermont Auvergne, INSERM, U1107, NEURO-DOL, F-63000, Clermont-Ferrand, France.
2. Université Clermont Auvergne, INRA, UNH, INRAE, UMR1019, UNH, F-63000 Clermont-Ferrand and F-63122 Saint-Genès Champanelle, France.
3. CHU Clermont-Ferrand, Direction de la recherche clinique et de l'innovation, F-63000, Clermont-Ferrand, France.
4. School of Pharmacy, Faculty of Science, University of East Anglia, UK.
5. Université Clermont Auvergne, INRA, UMR1019, UNH, CRNH Auvergne, F-63000, Clermont-Ferrand, France
6. Université Clermont Auvergne, INSERM U1107, NEURO-DOL, CHU Clermont-Ferrand, Laboratoire de Pharmacologie et de Toxicologie, F-63000, Clermont-Ferrand, France.
7. Université Clermont Auvergne, INSERM U1107, NEURO-DOL, CHU Clermont-Ferrand, Direction de la recherche clinique et de l'innovation, F-63000, Clermont-Ferrand, France.

Corresponding author:
Aurore Collin
INSERM U1107 NEURO-DOL
TSA 50400
28 Place Henri Dunant
63000 CLERMONT-FERRAND cedex 1
aurore.collin@uca.fr
+33 (0)4 73 17 80 41

Abstract

Among postmenopausal women with estrogen receptor-positive breast cancer, more than 80% receive hormone therapy including aromatase inhibitors (AIs). Half of them develop chronic arthralgia - characterized by symmetric articular pain, carpal tunnel syndrome, morning stiffness, myalgia and a decrease in grip strength - which is associated with treatment discontinuation. Only a few animal studies have linked AI treatment to nociception, and none to arthralgia. Thus, we developed a new chronic AI-induced nociceptive disorder model mimicking clinical symptoms induced by AIs, using subcutaneous letrozole pellets in ovariectomized (OVX) rats. Following plasma letrozole dosage at the end of the experiment (day 73), only rats with at least 90 ng/mL of letrozole were considered significantly exposed to letrozole (OVX+high LTZ group), whereas treated animals with less than 90 ng/mL were pooled in the OVX+low LTZ group. Chronic nociceptive disorder set in rapidly and was maintained for more than 70 days in the OVX+high LTZ group. Furthermore, OVX+high LTZ rats saw no alteration in locomotion, myalgia or experimental anxiety during this period. Bone parameters of the femora were significantly altered in all OVX rats compared to Sham+vehicle pellet. A mechanistic analysis focused on TRPA1, receptor suspected to mediate AI-evoked pain, and showed no modification in its expression in the DRG. This new long-lasting chronic rat model, efficiently reproduces the symptoms of AI-induced nociceptive disorder affecting patients' daily activities and quality-of-life. It should help to study the pathophysiology of this disorder and to promote the development of new therapeutic strategies.

Keywords: Arthralgia; Myalgia; Letrozole; TRPA1; Rat

Abbreviations: AIs, aromatase inhibitors; ANOVA,One-way analysis of variance; DRG, dorsal root ganglia; LTZ, letrozole; OVX, ovariectomized; PLT, pellets; REM, random-effects models; VEH, vehicle

Acknowledgements: None

Funding: This research did not receive any specific grant from funding agencies in the public, commercial, or not-for-profit sectors.

Conflict of interest: The authors declare that there is no conflict of interest

64 # 1. Introduction

65 Breast cancer is the most prevalent cancer among women. In the United States of
66 America, 3.8 million women are living with a history of invasive breast cancer, and 268,600
67 women were newly diagnosed in 2019 (Miller et al., 2019). This cancer has a good survival
68 rate thanks to routine screening and to codified therapeutic management, offering real chances
69 of survival to patients (Niravath, 2013). Thus 5-year, 10-year, and 15-year relative survival
70 rates for breast cancer are 89%, 83%, and 78%, respectively (Miller et al., 2016). About 79%
71 of postmenopausal patients with hormone-receptor positive [estrogen receptor-positive
72 (ER+)] breast cancer, regardless of the stage of the cancer, receive hormone therapy including
73 aromatase inhibitors (AIs) (Miller et al., 2016). AIs include non-steroidal inhibitors
74 (anastrozole and letrozole - LTZ) and a steroidal inhibitor (exemestane) (Gaillard and Stearns,
75 2011). Randomized clinical trials demonstrated that these AIs, anastrozole (Jakesz et al.,
76 2005), LTZ (Breast International Group (BIG) 1-98 Collaborative Group et al., 2005) and
77 exemestane (Coombes et al., 2004), were superior to tamoxifen alone, a selective estrogen
78 receptor modulator, in reducing breast cancer recurrence in postmenopausal patients with
79 early hormone-sensitive breast cancer. There were significantly fewer thromboembolic and
80 gynecologic adverse events with AI treatments than with tamoxifen (Coombes et al., 2004;
81 Breast International Group (BIG) 1-98 Collaborative Group et al., 2005; Jakesz et al., 2005).
82 Currently, AI adjuvant therapy is given for at least 5 years, but extending treatment to 10
83 years would be beneficial for patients, and produce higher rates of disease-free survival and a
84 lower incidence of contralateral breast cancer (Goss et al., 2016).

85 However, half of postmenopausal patients treated with AIs develop arthralgia,
86 characterized by symmetric joint pain (wrist, hands and knees), carpal tunnel syndrome,
87 morning joint stiffness, myalgia, back pain, osteoporosis and a decrease in grip strength (Din
88 et al., 2010; Siegel et al., 2012; Niravath, 2013; Mamounas et al., 2019). These symptoms

usually appear after 1.6 months and reach a peak 6 months after starting the treatment (Henry et al., 2008). Symptoms of AI-induced arthralgia severely affect patients' daily activities and quality-of-life and lead to poor compliance (Cella et al., 2006). Non-compliance with AI treatments progressively increases each year to reach 21%-38% in the third year of treatment (Partridge et al., 2008). In these non-compliant patients, non-compliance being due to intolerance, the leading cause (75% of non-compliant patients) is AI-associated musculoskeletal disorders (Henry et al., 2012). The underlying mechanisms of AI-associated musculoskeletal disorders still remain unknown and there is little effective treatment (Bhatnagar, 2007; Niravath, 2013; Robarge et al., 2016), apart from duloxetine, which significantly improves joint pain within 12 weeks of treatment compared to the placebo (Henry et al., 2018).

Preclinical studies in rodents have been developed to evaluate disorders induced by AI treatments relating to neurotransmission and cognition (Aydin et al., 2008), hormonal and lipid status (Evrard and Balthazart, 2004a, 2004b; Kumru et al., 2007; Ortega et al., 2013; Boutas et al., 2015; De Logu et al., 2016) as well as bone mineral density (Gasser et al., 2006; Kumru et al., 2007; Mohamed and Yeh, 2009). Few studies have linked AI treatment to nociception (Moradi-Azani et al., 2011; Fusi et al., 2014; Robarge et al., 2016), and to the best of our knowledge none have specifically examined arthralgia. Furthermore, some features of these studies are far-removed from clinical practice (e.g. use of male animals, intraplantar injections, short-term treatments) and limit the translational aspect. Regarding potential pathophysiological mechanism of AI-induced nociceptive disorders, TRPA1, a key receptor involved in hyperalgesia, and in neurogenic and chronic inflammation (Boutas et al., 2015), was recently shown to be involved in LTZ-induced pain (Fusi et al., 2014; De Logu et al., 2016).

Considering the clinical importance of AI-induced arthralgia, the inadequacy of current animal models, and the need for both pathophysiological exploration and pharmacological innovation, we developed a new model of chronic AI-induced chronic nociceptive disorder in order to mimic clinical symptoms induced by AIs. Given that the target pathology occurs in postmenopausal women, that sex-related hormonal status impacts pain and analgesic responses, suggesting that systemic estrogens may be negative regulators of pain (Tsao et al., 1999; Fillingim and Ness, 2000), we used ovariectomized (OVX) Sprague-Dawley female rats, in which a subcutaneous LTZ pellet was implanted. The main result we achieved is joint hypersensitivity that mimics AI-induced nociceptive disorder for a sustained period, with onset after 10 days and which is maintained significantly for more than 70 days, and involves alteration of bone architectural parameters.

2. Materials and methods

2.1. Animals

Experiments were conducted on female Sprague-Dawley rats (11 weeks old upon arrival, Janvier Labs, France). The animals were housed 3 per cage, with water and food *ad libitum*, exposed to a 12:12 h light/dark cycle and 50% hygrometry. The procedures were approved by the local ethics committee (C2E2A – Comité d'Ethique en Expérimentation Animale en Auvergne) and received the following authorizations: APAFIS#3409-2015123016491662v3 (July 25, 2017, Ministère de l'Enseignement Supérieur, de la Recherche et de l'Innovation, France). The experiments were carried out according to the ARRIVE guidelines for animal research (Kilkenny et al., 2010). Animals were daily observed in order to address animal welfare standards and animal weight was measured on days -13, 0, 7, 14, 21, 28, 35, 42, 49, 56, 63 and 70. Two investigators blinded to the treatments performed the behavioral tests (D.B.: ankle pressure test and muscle pressure test; J.V.: open field test and rotarod test). The treatment allocation was revealed at the end of the behavioral experiments. Four groups of

139 animals were used: OVX rats implanted either with subcutaneous LTZ pellets (OVX+PLT
140 200 and 400 µg/day) or vehicle pellets (OVX+VEH) (control group) and sham rats
141 (Sham+VEH). Treatment groups were randomized within cages (3 animals per cage) using a
142 permutation table, and the experiments were repeated 3 times, to achieve the following total
143 number of animals: Sham+VEH = 14 rats, OVX+VEH = 14 rats, OVX+PLT 200 = 14 rats,
144 and OVX+PLT 400 15 rats (1st experiment: Sham+VEH = 3 rats, OVX+VEH = 4 rats,
145 OVX+PLT 200 = 3 rats, and OVX+PLT 400 = 4 rats; 2nd experiment: Sham+VEH = 5 rats,
146 OVX+VEH = 5 rats, OVX+PLT 200 = 6 rats, and OVX+PLT 400 = 5 rats ; 3rd experiment:
147 Sham+VEH = 6 rats, OVX+VEH = 5 rats, OVX+PLT 200 = 5 rats, and OVX+PLT 400 = 6
148 rats). The results of the three experiment repetitions were pooled for the final analysis.
149

150 **2.2. Ovariectomy**

151 In order to mimic a postmenopausal status, females were ovariectomized at the age of
152 12 weeks to ensure good hormonal impregnation with full sexual maturity. Animals received
153 general anesthesia by single administration of xylazine / ketamine (10 mg/kg / 80 mg/kg, by
154 intraperitoneal injection). Analgesia was obtained with administrations of meloxicam (2
155 mg/kg, subcutaneous injection) during anesthesia and 24 hours after the surgery. Animals
156 were placed in ventral decubitus on a warming carpet, with ocular gel instilled into each eye
157 at the beginning of the surgery. Antisepsis was ensured with 70° alcohol and povidone iodine
158 disinfection of the skin. Incision (1.5 cm) was performed dorsally on the lumber part of the
159 back and the muscles were separated from one side. The ovaries were externalized, ligatured
160 (Vicryl 3/0) and cut. The muscles were sutured (Vicryl 3/0). Surgery was repeated on the
161 opposite side. Finally, the skin incision was sutured (Vicryl 3/0). Animal waking was
162 monitored individually in separate cages on a warming carpet. Three animals were placed

163 together in the same cage after complete locomotor activity recovery. Animals were
164 monitored every day during 3 days.
165
166 **2.3. Letrozole (LTZ) pellet implantation**
167 One week after surgery (day 0, Figure 1), all the animals underwent subcutaneous
168 insertion of a slow release pellet (Innovative Research of America, Sarasota, USA) of LTZ
169 (Leancare limited, Flintshire, United Kingdom) or vehicle. Under 3% isoflurane anesthesia,
170 the pellet (LTZ or vehicle) was subcutaneously inserted in the left jugular gutter, after a small
171 incision closed with Vicryl 3-0. Each pellet was estimated to release 200 and 400 µg of LTZ
172 per day over 90 days. The doses were chosen according to the studies of Kafali *et al.* (Kafali
173 et al., 2004) and Ortega *et al.* (Ortega et al., 2013) using the same type of pellets. LTZ
174 treatment was maintained for 73 days in order to maintain a chronic LTZ exposure similar to
175 human therapy (73 days of treatments in rat can be extrapolated to 4.9-7.3 years of treatment
176 in human (Sengupta, 2013).
177
178 **2.4. Biological monitoring of letrozole (LTZ)**
179 On day 73, animals were euthanized and blood collected to determine LTZ plasma
180 concentration (Figure 1).
181 A stock solution of LTZ and phenobarbital D5 (internal standard, IS) was prepared at
182 1 g/L in methanol. All standard solutions were stored at -20°C. Working solutions of LTZ
183 were prepared at 5 mg/L, 500 µg/L and 50 µg/L in methanol and the internal standard was 50
184 mg/L in water.
185 The extraction procedure was based on the method previously validated by Roche *et*
186 *al.* (Roche et al., 2016). Height points of calibration curves were constructed in the
187 concentration ranges of 1 – 1000 µg/L as well as different quality control (1, 40, 400 and

188 1000 µg/L). Before purification on-line, 10 µL of IS was added to 200 µL of sample solutions
189 (standards, controls and samples) and proteins were precipitated with 200 µL of acetonitrile
190 and 40 µL of methanol. The samples were vortexed vigorously for 10 min at room
191 temperature and centrifuged for 10 min at 14,000 rpm at 4 °C. The supernatant was then
192 transferred into a vial.

193 Twenty microliters of standard, control or sample preparation were injected into liquid
194 chromatography systems (transcend TLX 1, Thermo Fisher, San Jose, USA). On-line
195 chromatography purification was carried out using three Turboflow® purification columns in
196 series: a Cyclone P, a Cyclone MAX and a C18 XL (0.5 x 50 mm, Thermo Fisher). The
197 chromatographic column was a Betasil® phenyl/hexyl 100 x 3 mm with a particle size of 3
198 µm. The analytical column was set at 30 °C. A gradient system with the mobile phase
199 consisting of solvent A (0.1%; v/v; formic acid in water) and solvent B (1%; v:v; formic acid
200 in acetonitrile) was set at a flow rate of 300 µL/min. The chromatographic run lasted 33.58
201 min. During the first 3 min, the sample was purged through the divert valve. Acquisition by
202 the mass detector was performed over the following 30.58 min.

203 The MS analysis was performed using a Thermo Scientific Exactive benchtop
204 Orbitrap® instrument, driven by Xcalibur® software (version 2.2 SP1). We used a heated
205 electrospray ionization source (HESI II). The compounds were ionized by the source in
206 negative mode. The desolvation temperature was set at 350 °C, the curtain gas rate at 40 AU
207 (arbitrary units), auxiliary gas flow at 8 AU, the ionization voltage was set at 3 kV and the
208 capillary temperature at 250 °C. Acquisition used "fullscan" mode over a wide range of
209 masses (m/z): 200–300 amu in negative modes at a resolution of 50,000 (FWHM). Extract
210 mass was achieved at 10 ppm for LTZ (m/z=284.09399) and for internal standard
211 (m/z=236.10890). The concentrations of LTZ were determined by their area ratios to that of

212 the IS using a weight quadratic fit. The lower limit of quantification (LLOQ) of LTZ was 1
213 µg/L and the upper limit of quantification (ULOQ) was 1,000 µg/L in plasma.
214
215 **2.5. Behavioral tests**
216 *2.5.1. Ankle pressure test*
217 An ankle pressure test was performed weekly throughout the study on day 1, 10, 17,
218 22, 30, 38, 45, 52, 59, 66, 72, and for each experiment repetition (Figure 1). Nociceptive
219 thresholds were assessed by applying increasing pressure on the right hind ankle until the
220 animals squeaked or struggled, using a paw-pressure test loaded with a 30 g weight and using
221 the flat part of the tip (Randall-Selitto test, Bioseb, France). The maximum pressure applied to
222 the animal's paw was 450 g. The vocalization or struggle threshold was measured 2 or 3 times
223 in order to obtain 2 consecutive values that did not differ by more than 10%, and leaving at
224 least a 5-min interval between 2 measurements. The results are expressed, by the mean of the
225 2 closest values, in grams (g) and compared to baseline.
226
227 *2.5.2. Muscle pressure test*
228 A muscle pressure test was performed weekly throughout the study on day 0, 9, 16,
229 23, 31, 31, 37, 44, 52, 58, 65, 72, and for each experiment repetition (Figure 1). Nociceptive
230 thresholds (grams) were assessed by applying increasing pressure on the left thigh (*biceps*
231 *femoris, semitendinosus* and *semimembranosus*) of the animals using a portative pressure
232 device (Smalgo, Bioseb, France) (Kim et al., 2011) until they squeaked or struggled. The
233 maximum pressure applied to the animal's paw was 800 g. The vocalization or struggle
234 threshold was measured 2 or 3 times in order to obtain 2 consecutive values that did not differ
235 by more than 10%, and leaving at least a 5-min interval between 2 measurements. The results
236 are expressed, by the mean of the 2 closest values, in grams (g) and compared to baseline.

237

238 *2.5.3. Open field test*

239 An open field test was performed at day 49 after pellet implantation (approximately
240 half of letrozole treatment), and for each experiment repetition (Figure 1). Rats were placed
241 alone in the center of a square arena (90 x 90 cm, height 45 cm) made of opaque plastic,
242 without any prior habituation, and were left alone for 5 minutes. Light intensity at the center
243 of the open field was 30 lux. A camera was mounted directly above the field to record the
244 animal's behavior. Each recording was analyzed with a specific software (EthoVision®,
245 France). The total distance travelled, mean speed, and time spent in the inner zone were
246 counted. The open field was cleaned after each rat was tested.

247

248 *2.5.4. Rotarod test*

249 A rotarod test was performed weekly throughout the study on day 8, 15, 22, 29, 38, 43,
250 51, 57, 64 and 73, and only for the two first experiment repetitions (Figure 1). Motor
251 coordination was assessed using an accelerating rotarod (Bioseb, France). Motor coordination
252 was defined as a rat's ability to stay on a rotating rod as the acceleration speed increased
253 constantly from 4 to 40 rpm over 5 min. Before the beginning of the experiments, the rats
254 were trained gradually to stay on the fixed rod for 5 min on 2 consecutive days, and then on
255 the rotating rod (4 rpm) for 5 min on a further 2 days. The length of time that each rat was
256 able to stay on the rotating rod was measured 2 or 3 times in order to obtain 2 values that did
257 not differ by more than 10%, and leaving at least a 10-min interval between 2 measures. The
258 results are expressed, by the mean of the 2 closest values, in seconds (s) and compared to
259 baseline.

260

261 **2.6. Evaluation of bone architectural parameters**

262 Bone femora architectural parameters were quantified at necropsy at day 73, and only
263 for the second experiment repetition (day 73, Figure 1). Micro-computed tomography scans
264 (eXplore CT 120, GE Healthcare, Fairfield, CT) were performed on the dried distal femurs.
265 Bone mineral density of the metaphyseal trabecular bones was estimated as the mean
266 converted grayscale level within the region-of-interest of trabecular bone. Bone volume
267 fraction of the femora (BV/TV), bone volume ratio (BS/TV), trabecular thickness (Tb.Th),
268 trabecular separation (Tb.Sp), trabecular number (Tb.N), trabecular bone pattern factor
269 (Tb.Pf), degree of anisotropy (DA), and structure model index (SMI) were evaluated using
270 MicroView Advanced Bone Analysis software (GE Healthcare, Fairfield, CT).
271
272 **2.7. Protein expression analyses**
273 At day 73 (Figure 1), dorsal root ganglia (DRG) from L4 to L6 were rapidly removed
274 in euthanized animals and snap frozen in liquid nitrogen then stored at -80°C until analysis.
275 Proteins were extracted in lysis buffer pH 7.5 containing 50 mM HEPES, 150 mM NaCl, 10
276 mM EDTA, 10 mM Tetra-sodium pyrophosphate decahydrate, 2 mM vanadate, 100 mM
277 sodium fluoride, 0.5mM phenylmethanesulfonylfluoride, 100 UI/mL aprotinin, 20 µM
278 leupeptin and 1% triton. Whole-cell lysates were titrated to determine total protein
279 concentrations using a BCA Protein Assay kit (Pierce). For western immunoblotting,
280 Laemmli loading buffer was added to the samples containing an equal weight of total proteins
281 (50 µg) and heated at 95°C for 5 min. After separation by SDS-PAGE using 10% acrylamide
282 gels, the proteins were transferred to nitrocellulose membranes using a Bio-Rad wet blotting
283 system. The membranes were then blocked for 1h in 5% nonfat milk in TBS 1X at room
284 temperature. For TRPA1 (Santa-Cruz) and β-actin (Sigma-Aldrich) detection, antibodies at
285 1:500 and 1:5,000 respectively were added and the mixture was incubated overnight at 4°C on
286 a rotating plate. After washing with 0.1% TBS-T solution, the membranes were probed with

287 appropriate HRP-conjugated secondary antibodies diluted at 1:10,000 in 5% nonfat dry milk
288 in TBS 1X for 1h at room temperature. Blots were finally quantified by densitometric analysis
289 using Bio-Rad imaging software (Chemidoc). The TRPA1 bands of each sample were
290 normalized relative to the corresponding β-actin band.
291

292 **2.8. Statistical method and analysis**

293 The sample size estimation was calculated according to effect-size bounds
294 recommended by Cohen's (Cohen, 1988): small (ES: 0.2), medium (ES: 0.5) and large (ES:
295 0.8, "grossly perceptible and therefore large"). More precisely, with a minimum of 14 animals
296 with at least 10 repeated measures, relevant effect-size greater than 0.5 can be highlighted for
297 a two-sided type I error at 0.008 (correction due to multiple comparisons), a statistical power
298 greater than 80% and an intra-individual correlation coefficient at 0.05. For example, for the
299 ankle pressure test, it corresponds to show a minimal difference between groups of 15%
300 change for a standard-deviation equals 30%.

301 For behavioral tests, means and standard error of the mean (SEM) were calculated for
302 quantitative variables. Normality of distribution was verified by a Shapiro-Wilk test. To
303 compare the time-course evolution of different parameters, a repeated-measure ANOVA (or a
304 non-parametric Friedman test if necessary) was followed by a Tukey-Kramer test to compare
305 differences between and within groups. If a significant interaction between time and group
306 was observed, a one-way ANOVA was performed for all time points. These analyses were
307 completed by random-effects models (REM), considered more robust to missing data
308 (Verbeke and Molenberghs, 2009). The REM were able to take into account 1) fixed effects
309 as treatment, time and interaction between time and group, and 2) random subject effects as
310 random intercept and slope. Residual normality was checked for all models presented in this
311 article. For multiple comparison with no repetition of the assessed variable, a Kruskal-Wallis

312 non-parametric test was performed followed by a post hoc Dunn test. Results from
313 immunoblotting were analyzed using a nonparametric Mann-Whitney-Wilcoxon test to
314 compare differences between groups. Differences were considered statistically significant at
315 $p<0.05$. Statistical analysis was performed using STATA® v.10 software (StataCorp, College
316 Station, TX, USA).
317

318 # 3. Results

319 ## 3.1. Determination of LTZ exposed-rats

320 We hypothesized that all the rats could not be equally exposed to LTZ. Therefore, in
321 order to check rat exposure, the LTZ endpoint concentration was measured in plasma to point
322 out which rats could be selected to ensure a rigorous and relevant model of AI-induced
323 chronic nociceptive disorder (**Figure 2A**). However, several animals of the groups OVX+PLT
324 200 and OVX+PLT 400 had very low concentrations of LTZ at day 73 after the pellet
325 implantation. Rats were considered highly exposed to LTZ for plasma concentrations above
326 90 ng/ml. Postmenopausal women with breast cancer after 1 month of LTZ treatment (2.5 mg
327 daily) have a median plasma concentration of LTZ of 89.7 ng/ml (range: 28.4–349.2 ng/ml;
328 n=280 patients) (Desta et al., 2011). Consequently, rats with at least 90 ng/mL of LTZ were
329 pooled in the OVX+high LTZ group (n=11; $p<0.001$) (**Figure 2B**), with a mean plasma
330 concentration of LTZ of 424.4 ± 183.9 ng/ml. Accordingly, treated animals with less than 90
331 ng/mL of LTZ were pooled in an OVX+low LTZ group (n=18, mean plasma concentration of
332 LTZ: 9.7 ± 11.5 ng/ml). In the OVX+high LTZ group, no difference in plasma LTZ
333 concentrations was recorded between animals implanted with a 200 µg/day LTZ pellet and a
334 400 µg/day LTZ pellet (334.8±130.6 *vs* 531.9±191.8 ng/mL, p=0.12).
335

336 ## 3.2. Effect of chronic LTZ treatment on rat body weight and locomotion

337 From day 42 until day 70 (last weight measurement), OVX+VEH animals gained
338 significantly more weight than Sham+VEH animals (from +5.6% to +9.6%, $p<0.05$ and
339 $p<0.001$, respectively) (**Figure 3**). The same results were recorded for OVX+low LTZ and
340 OVX+high LTZ compared to Sham+VEH animals (for OVX+low LTZ from days 35 to 70:
341 +7.7% to +11.1%, $p<0.05$ and $p<0.001$; for OVX+high LTZ from days 49 to 70: +4.5% to
342 +8.6%, $p<0.01$ and $p<0.01$, respectively) (**Figure 3**). No difference in weight was recorded
343 between OVX+VEH, OVX+low LTZ and OVX+high LTZ animals. The same results were
344 recorded for the initial treatment allocation (OVX+PLT 200 and 400 µg/day) (supplementary
345 file, Figure 3S).

346 To determine whether chronic LTZ treatment altered rat locomotion, gait activity was
347 evaluated with the rotarod test (**Figure 4A**). Rat performances on rotarod were not modified
348 in the LTZ-group compared to the control group ($p>0.05$). Furthermore, locomotion activity
349 (distance and velocity) and experimental anxiety (time spent in the inner zone) were assessed
350 with an open field test, at day 49 following implantation of the pellet. Locomotion activities
351 were not affected by LTZ treatment (**Figure 4B**). Finally, the time spent in the inner zone of
352 the open field was the same in all groups (**Figure 4C**), showing that neither OVX nor LTZ
353 induced anxiety-like behavior. The same results were recorded for the initial treatment
354 allocation (OVX+PLT 200 and 400 µg/day) (supplementary file, Figure 4S).

355

356 **3.3. Evaluation of nociceptive disorders**

357 In order to evaluate nociceptive disorders, pain thresholds were measured on ankle and
358 muscle, respectively. Pain ankle thresholds were not different between Sham+VEH and
359 OVX+VEH animals, except at day 10 ($p=0.039$). Pain ankle thresholds were not different
360 between Sham+VEH, OVX+low LTZ and OVX+high LTZ animals, throughout the
361 experiment. For OVX+low LTZ animals, pain ankle thresholds were lower than for

362 OVX+VEH at day 10 (p=0.032) and 17 (p=0.049), and thereafter remained not different until
363 the end of the experiment. For OVX+high LTZ animals, pain ankle thresholds were lower
364 than OVX+VEH, starting from day 10 (p=0.002) until day 72 (p=0.018), except on day 66.
365 The maximal decrease in pain thresholds was observed on day 38 (-27.8%). Pain ankle
366 thresholds were also lower in OVX+high LTZ animals compared to OVX+low LTZ animals
367 on day 30 (p=0.032), and from day 59 until day 72 (p=0.041 and p=0.03, respectively). The
368 area under the time course curve of pain thresholds was lower (-24% decrease) for OVX+high
369 LTZ animals compared to OVX+VEH (**Figure 5A**). Considering the initial treatment
370 allocation, pain ankle thresholds were not different between OVX+VEH, OVX+PLT 200 and
371 OVX+PLT 400 (supplementary file, Figure 5S).

372 Results did not reveal the development of significant long-term myalgia in LTZ-
373 treated rats (**Figure 5B**). The same results were recorded for the initial treatment allocation
374 (OVX+PLT 200 and 400 µg/day) (supplementary file, Figure 5S).

375

376 **3.4. Evaluation of bone architectural parameters**

377 Bone parameters (BV/TV, BS/TV, Tb.Th, Tb.Sp, Tb.N, Tb.Pf, DA and SMI) were
378 assessed by micro-computed tomography performed on femora at day 73 (**Table 1**). Among
379 these parameters, BV/TV, BS/TV and Tb.N were significantly reduced in all OVX animals
380 (OVX+VEH, OVX+low LTZ and OVX+high LTZ) compared to Sham+VEH animals. Tb.Sp,
381 Tb.Pf and SMI were significantly increased in all OVX animals (OVX+VEH, OVX+low LTZ
382 and OVX+high LTZ) compared to Sham+VEH animals. No significant difference was found
383 between OVX+VEH *versus* OVX+low LTZ and OVX+high LTZ animals, demonstrating the
384 impact of ovariectomy in these alterations. However, Tb.Th was significantly reduced only
385 for OVX+low LTZ and OVX+high LTZ animals in comparison to Sham+VEH animals,
386 suggesting that LTZ treatment exacerbated trabecular thickness due to ovariectomy. The same

387 results were recorded for the initial treatment allocation (OVX+PLT 200 and 400 µg/day)
388 (supplementary file, Table1S).
389
390 **3.5. Effect of letrozole (LTZ) on protein expression of TRPA1**
391 To investigate whether LTZ affects the expression of TRPA1, a key receptor involved
392 in hyperalgesia, neurogenic and chronic inflammation (Basso and Altier, 2017), western blot
393 was performed in DRG (**Figure 6**). TRPA1 expression in the OVX+high LTZ group was not
394 significantly modified compared to OVX+VEH (p=0.20), demonstrating that TRPA1
395 expression was independent of LTZ.
396
397 # 4. Discussion
398 Half of postmenopausal patients treated with AI develop arthralgia, as well as back or
399 muscle pain, and joint stiffness, which are associated with poor compliance with treatment
400 (Henry et al., 2012; Mamounas et al., 2019). This disabling adverse effect of AIs prompted us
401 to further investigate and develop a new clinically-relevant animal model of chronic AI-
402 induced arthralgia. To this end, we: (1) worked with ovariectomized rats since AIs are
403 administered to postmenopausal women (Miller et al., 2016), (2) explored the nociceptive
404 sensitivity of joints to mimic clinical symptomatology as far as possible (Niravath, 2013), (3)
405 performed a longitudinal study taking into account the chronicity of the disorder (Bao et al.,
406 2018) by ensuring prolonged treatment with pellets already used to deliver estradiol to rats
407 (Mosquera et al., 2015; Gérard et al., 2017), (4) explored the state of the bone structure known
408 to be altered in patients treated with AIs (Pineda-Moncusí et al., 2018), (5) explored the
409 nociceptive sensitivity of muscles, potentially affected in patients (Nabieva et al., 2019) and
410 motor activity that may be altered by arthralgia (Brown et al., 2014), (6) added an exploration

411 of anxiety-like behavior, as psychological distress can be reported in cancer patients under
412 endocrine therapy (de Bock et al., 2012).

413 The use of LTZ pellets and the willingness to monitor its effects on different
414 parameters over time required an essential prior analysis of LTZ diffusion from the pellets.
415 Based on end-point plasma concentrations of LTZ, we identified two groups of animals [high
416 plasma concentrations of LTZ (OVX+high LTZ) and low plasma concentrations of LTZ
417 (OVX+low LTZ) groups], either higher or less than 90 ng/ml. This threshold value was
418 chosen according to the mean LTZ plasma concentration in postmenopausal women with
419 breast cancer after 1 month of a 2.5 mg daily dose (median plasma concentration: 89.7 ng/ml)
420 (Desta et al., 2011). On the other hand, it is difficult to compare our data with that in the
421 rodent literature because these experiments were performed after a single administration.
422 Thus, in rats treated with a 2 mg/kg oral dose, maximal concentration of LTZ was 674 ng/ml,
423 6h after administration (Liu et al., 2000), while in mice, a level of 55.3±4.8 ng/ml was
424 obtained 1 hour after an oral dose of 0.5 mg/kg (De Logu et al., 2016). The LTZ pellets (200
425 and 400 µg/day) used in our study, correspond to 0.7 and 1.4 mg/kg daily doses at the
426 beginning of the experiment (mean weight of OVX animals ≈ 290 g), and 0.5 and 1 mg/kg
427 daily doses at the end (mean weight of OVX animals ≈ 400 g). In the OVX+high LTZ groups,
428 mean plasma concentrations were around 424.4 ± 183.9 ng/ml, i.e., values within a range of
429 levels broadly comparable to those obtained in the previous studies performed in rodents, but
430 with the advantage of prolonged impregnation over a long period of time.

431 Thus behavioral or histological studies were carried out by distinguishing between
432 these two groups and comparing them with the OVX group treated with the vehicle
433 (OVX+VEH) to evaluate the impact of LTZ; the sham group (Sham+VEH) enabled us to
434 evaluate the impact of ovariectomy and that of its association with LTZ.

435 Under these conditions, we demonstrated articular hyperalgesia in the animals with the
436 highest LTZ concentrations (OVX+high LTZ), whereas hyperalgesia only occurred for two
437 days in animals with lower LTZ concentrations (OVX+low LTZ). In the OVX+high LTZ
438 group, articular hyperalgesia was maintained throughout the experiment with a 24% average
439 decrease, as shown by the comparison of the areas under the time course curve of pain
440 thresholds, compared to OVX+VEH animals. Thus, the objective to reproduce the joint pain
441 disorder observed in patients treated with AI in animals is achieved, and the extent of the
442 resulting articular hyperalgesia will allow subsequent pathophysiological and
443 pharmacological studies to be carried out.

444 Robarge *et al.* showed that a single oral dose of LTZ (1 and 5 mg/kg) induced
445 sustained tactile allodynia (von Frey test on hind paw) but not thermal hyperalgesia
446 (Hargreaves test) in ovariectomized rats (Robarge et al., 2016). They also demonstrated the
447 same results after oral daily doses of LTZ (5 mg/kg) for 15 days, but in male rats (Robarge et
448 al., 2016). De Logu *et al.* and Fusi *et al.* demonstrated that a single oral dose of LTZ (0.5
449 mg/kg) induced tactile allodynia (von Frey test on hind paw) in male mice (Fusi et al., 2014;
450 De Logu et al., 2016). In pain models, daily intrathecal infusion of LTZ (1 mg/kg) for 28 days
451 enhanced tactile allodynia (von Frey test on hind paw) induced by a spinothalamic tract injury
452 in female rats (non ovariectomized) (Ghorbanpoor et al., 2014). A subcutaneous injection of
453 LTZ (5 mg/kg) before subcutaneous plantar injection of formalin (0.25%) increased the pain
454 scores in ovariectomized rats (Moradi-Azani et al., 2011). However, these studies raise the
455 question of extrapolation to the clinical situation. Indeed, the question of sex and the role of
456 estrogens and the effect of LTZ in the long-term arises, as AIs are used for the prolonged
457 management of hormone-responsive breast cancer in postmenopausal women (Din et al.,
458 2010). Sex-related hormones are implicated in pain and analgesic response in clinical and
459 preclinical studies, and estrogen administration leads to an antinociceptive effect in animal

460 models of pain, suggesting that systemic estrogens may be negative regulators of pain (Tsao
461 et al., 1999; Fillingim and Ness, 2000). Moreover, some studies underlined specific
462 mechanisms of ovarian steroids exerted on opioid systems directly, depending on the
463 treatment duration (Ratka and Simpkins, 1991). However, it is also clear that the relationship
464 between sex steroid hormones and pain is complex, modulating the nervous system
465 functioning, as well as the pathophysiological processes themselves (Vincent and Tracey,
466 2008). Regarding the maintenance of plasma LTZ concentrations, previous studies described
467 LTZ concentrations as being more persistent in females than in males, following single oral
468 administration (Liu et al., 2000), and pharmacokinetic studies highlight that LTZ
469 concentration steady state (2.5 mg daily doses) was reached after 4 weeks of treatment (Pfister
470 et al., 2001). All these data highlight the need to work in females with continuous LTZ
471 treatment to faithfully transpose clinical symptoms induced by Ais.

472 Bone parameters of the femora were drastically altered in all OVX animals compared
473 to sham animals as already shown by other authors, and confirming the castration and the
474 estrogen deprivation (Goss et al., 2007; Rosales Rocabado et al., 2018). Only trabecular
475 thickness (Tb.Th) was decreased in LTZ treated animals (OVX+low LTZ and OVX+high
476 LTZ animals) but not in OVX+VEH animals, compared to sham animals. Thus, LTZ
477 treatment could exacerbate bone alteration induced by ovariectomy. In OVX rats, bone
478 mineral densities of the lumbar vertebra and femora were not changed after 16 weeks'
479 treatment with LTZ (oral daily dose of 1 mg/kg) compared to the control animals (Goss et al.,
480 2004, 2007). In the same way, bone parameters of the femora, Tb.Th, Tb.Sp, and Tb.N, were
481 not changed after the 16 weeks' treatment with LTZ (Goss et al., 2007). In women with
482 primary breast cancer, bone mineral density (hip and lumbar spine) was significantly
483 decreased after 24 months' treatment with LTZ in comparison to placebo group (Perez et al.,
484 2006). The incidence of fractures was highest among women treated with LTZ monotherapy

compared to women treated with tamoxifen monotherapy (BIG 1-98 Collaborative Group et al., 2009), but it was unchanged compared to placebo group (Goss et al., 2005). Thus, the limited bone changes observed in our study are consistent with the data in the literature. However, additional studies could be envisaged to better understand the bone disorders potentially induced by LTZ.

In this study, rats developed long-term nociceptive disorder (ankle pressure test) but not myalgia, and there was no alteration of locomotion. To our knowledge, no study has ever assessed AI-induced myalgia in rats or mice, and previous studies did not systematically report myalgia as a clinical symptom in patients (Din et al., 2010; Mamounas et al., 2019). Din et al. reported that aromatase inhibitor-induced arthralgia was increased by at least a factor of 2.5 compared to myalgia. Besides, clinical studies did not systematically monitor this side-effect (Din et al., 2010). In this study, LTZ did not alter rat locomotion assessed by the rotarod and open field tests. Similar results were previously observed on the locomotion of OVX rats treated with LTZ (daily intraperitoneal injection of 1 mg/kg for 8 days) when subjected to the open field test (Kokras et al., 2018).

No anxiety-like behavior was recorded using the open field test (e.g. decrease in the time spent in the inner zone) for the OVX+high LTZ rats. Similar results were found by Kokras *et al.* on the open field test and also with the forced swim test, used as a stressful procedure that elicits coping behaviors (Kokras et al., 2018). In non-ovariectomized female rats, LTZ had no effect on experimental anxiety assessed with the open-field and the elevated plus maze tests contrary to ovariectomized group (Renczés et al., 2020). The effect induced by ovariectomy on the open field test was also reported by Kokras *et al.* (Kokras et al., 2018). Other studies reported that ovariectomized mice treated with LTZ presented mild anxious behaviors (open-field and elevated plus maze tests) (Meng et al., 2011).

509 From a mechanistic point of view, we lastly assessed the expression of TRPA1, a key
510 receptor suspected to mediate AI-evoked pain (Fusi et al., 2014; De Logu et al., 2016) and
511 involved in neuropathic pain (Basso and Altier, 2017). We showed that TRPA1 expression
512 was slightly decreased in the DRG of OVX+high LTZ rats but not significantly compared to
513 OVX+VEH (p=0.20). In Fusi *et al.* (Fusi et al., 2014), AIs promote TRPA1-dependent
514 mechanical hypersensitivity and decreased forelimb grip force in mice. Furthermore, the
515 pronociceptive action of AIs was markedly attenuated in TRPA1-/- mice. Fusi *et al.* suggested
516 that the LTZ nociceptive effect could be linked to its potential ability to activate TRPA1
517 through a nitrile moieties structure, which may result in TRPA1 gating (Fusi et al., 2014).
518 However, the same research team demonstrated that the LTZ concentration required to engage
519 TRPA1 in mice was higher than those found in the plasma of patients, and suggested that
520 androstenedione could lower the LTZ concentration required to engage TRPA1 (De Logu et
521 al., 2016). Based on the literature data, we expected an increase in TRPA1 expression in
522 DRG. Indeed several publications reported that TRPA1 expression was upregulated in animal
523 models of neuropathic pain (traumatic neuropathy or chemotherapy-induced peripheral
524 neuropathy) (Giorgi et al., 2019). More recently, in a mouse model of endometriosis, LTZ
525 improved nociceptive behaviors of animals, with an increased TRPA1 channels expression in
526 dorsal root ganglion neurons and nerve fibers close to endometriosis lesions (Fattori et al.,
527 2020). Moreover, Wang *et al.* showed that TRPA1 expression (mRNA and protein) in
528 primary DRG cell cultures was increased by formaldehyde (TRAP1 agonist) and decreased by
529 menthol (TRPA1 antagonist) (Wang et al., 2019). However, previous studies showed TRPA1
530 channel pharmacological desensitization in sensory neurons due to agonists like mustard oil
531 or capsazepine (Akopian et al., 2007; Raisinghani et al., 2011; Kistner et al., 2016) and this
532 desensitization was shown to involve TRPA1 internalization regulated by TRPV1 (Akopian et
533 al., 2007). Such a mechanism could be a potential explanation as to the decrease in TRPA1

534 expression in our 73-day, long-term LTZ treatment model. Finally, to the best of our
535 knowledge, no data concerning TRPA1 expression in patients are available. Therefore, LTZ
536 and TRPA1 should be carefully interpreted and new investigations are required to clarify the
537 involvement of TRPA1.

538 This study presents several limitations that should be keep in mind for further
539 investigations. To mimic human menopause, as referred previously, animals were
540 ovariectomized but to be closer to human features, aged animals should be used. However, a
541 hallmark of human menopause is complete ovarian failure, that doesn't exist in rodents,
542 therefore the modeling of human menopause in rodents is still debating (Koebele and
543 Bimonte-Nelson, 2016). LTZ exposure was monitored at the final time point, but regular and
544 earlier monitoring of LTZ would be necessary when using this way of drug administration in
545 order to keep homogenous animal groups. Subcutaneous pellets, commonly used to deliver
546 estradiol (Mosquera et al., 2015; Gérard et al., 2017), were chosen to continuously provide
547 LTZ. The chronic dissolution of LTZ pellets could be easily extrapolated to a five-year
548 aromatase inhibitor therapy in human. This reliable and easily applicable pharmaceutical form
549 limits animal handling for characterizing our model (e.g. daily injections or gavage or blood
550 collections) and decrease probable concomitant bias in behavioral tests. To control hormonal
551 depletion owing to ovariectomy, estrogen plasma levels were not assessed but as expected, we
552 clearly detected estrogen deprivation effects in ovariectomized groups compared to sham
553 animals (e.g. significant chronic weight gain or final drastic alteration of bone architectural in
554 OVX animals). Behavioral tests (e.g. pressure-evoked pain) were used to determine chronic
555 nociceptive disorders (ankle pressure test) but not myalgia with no alteration in locomotion
556 (e.g. rotarod test, open field test). These tests may be potentially insufficient but was
557 associated with an evaluation of bones architectural parameters that are known to be clearly
558 affected by aromatase inhibitor treatment and correlated to pain (Gaillard and Stearns, 2011).

559 Moreover, histological/morphological explorations of the joints (ankle joint) would be
560 necessary to explore the pathophysiological changes induced by LTZ, and already described
561 in patients (Tenti et al., 2020). Finally, a pharmacological validation of this animal model
562 with duloxetine would be relevant. To this date, duloxetine is the only effective drug in
563 clinical trials (Henry et al., 2018).

564 In conclusion, since more than half of the patients developed arthralgia following AI
565 treatment, a new model of nociceptive disorder-related behavior in rodents deserved to be
566 developed. Thus, the model presented in this work seems to respond appropriately to this need
567 and may allow for subsequent pathophysiological and pharmacological studies.

568

569 **Supplementary files**

570 Figure 3S

571 Figure 4S

572 Figure 5S

573 Table 1S

574

575 **References**

576 Akopian, A. N., Ruparel, N. B., Jeske, N. A., and Hargreaves, K. M. (2007). Transient
577 receptor potential TRPA1 channel desensitization in sensory neurons is agonist
578 dependent and regulated by TRPV1-directed internalization. *J Physiol* 583, 175–193.
579 doi:10.1113/jphysiol.2007.133231.

580 Aydin, M., Yilmaz, B., Alcin, E., Nedzvetsky, V. S., Sahin, Z., and Tuzcu, M. (2008). Effects
581 of letrozole on hippocampal and cortical catecholaminergic neurotransmitter levels,
582 neural cell adhesion molecule expression and spatial learning and memory in female
583 rats. *Neuroscience* 151, 186–194. doi:10.1016/j.neuroscience.2007.09.005.

584 Bao, T., Seidman, A., Li, Q., Seluzicki, C., Blinder, V., Meghani, S. H., et al. (2018). Living
585 with chronic pain: perceptions of breast cancer survivors. *Breast Cancer Res. Treat.*
586 169, 133–140. doi:10.1007/s10549-018-4670-9.

587 Basso, L., and Altier, C. (2017). Transient Receptor Potential Channels in neuropathic pain.
588 *Curr Opin Pharmacol* 32, 9–15. doi:10.1016/j.coph.2016.10.002.

589 Bhatnagar, A. S. (2007). The discovery and mechanism of action of letrozole. *Breast Cancer*
590 *Res Treat* 105, 7–17. doi:10.1007/s10549-007-9696-3.

591 BIG 1-98 Collaborative Group, Mouridsen, H., Giobbie-Hurder, A., Goldhirsch, A.,
592 Thürlimann, B., Paridaens, R., et al. (2009). Letrozole therapy alone or in sequence
593 with tamoxifen in women with breast cancer. *N. Engl. J. Med.* 361, 766–776.
594 doi:10.1056/NEJMoa0810818.

595 Boutas, I., Pergialiotis, V., Salakos, N., Agrogiannis, G., Konstantopoulos, P., Korou, L.-M.,
596 et al. (2015). The impact of Anastrazole and Letrozole on the metabolic profile in an
597 experimental animal model. *Sci Rep* 5, 17493. doi:10.1038/srep17493.

598 Breast International Group (BIG) 1-98 Collaborative Group, Thürlimann, B., Keshaviah, A.,
599 Coates, A. S., Mouridsen, H., Mauriac, L., et al. (2005). A comparison of letrozole and
600 tamoxifen in postmenopausal women with early breast cancer. *N. Engl. J. Med.* 353,
601 2747–2757. doi:10.1056/NEJMoa052258.

602 Brown, J. C., Mao, J. J., Stricker, C., Hwang, W.-T., Tan, K.-S., and Schmitz, K. H. (2014).
603 Aromatase inhibitor associated musculoskeletal symptoms are associated with reduced
604 physical activity among breast cancer survivors. *Breast J* 20, 22–28.
605 doi:10.1111/tbj.12202.

606 Cella, D., Fallowfield, L., Barker, P., Cuzick, J., Locker, G., Howell, A., et al. (2006). Quality
607 of life of postmenopausal women in the ATAC ("Arimidex", tamoxifen, alone or in
608 combination) trial after completion of 5 years' adjuvant treatment for early breast
609 cancer. *Breast Cancer Res. Treat.* 100, 273–284. doi:10.1007/s10549-006-9260-6.

610 Cohen, J. (1988). *Statistical power analysis for the behavioral sciences*. 2nd ed. Hillsdale,
611 N.J: L. Erlbaum Associates.

612 Coombes, R. C., Hall, E., Gibson, L. J., Paridaens, R., Jassem, J., Delozier, T., et al. (2004). A
613 randomized trial of exemestane after two to three years of tamoxifen therapy in

614 postmenopausal women with primary breast cancer. *N. Engl. J. Med.* 350, 1081–1092.
615 doi:10.1056/NEJMoa040331.

616 de Bock, G. H., Musters, R. F., Bos, H. J., Schröder, C. P., Mourits, M. J. E., and de Jong-van
617 den Berg, L. T. W. (2012). Psychotropic medication during endocrine treatment for
618 breast cancer. *Support Care Cancer* 20, 1533–1540. doi:10.1007/s00520-011-1242-5.

619 De Logu, F., Tonello, R., Materazzi, S., Nassini, R., Fusi, C., Coppi, E., et al. (2016). TRPA1
620 Mediates Aromatase Inhibitor-Evoked Pain by the Aromatase Substrate
621 Androstenedione. *Cancer Res.* 76, 7024–7035. doi:10.1158/0008-5472.CAN-16-1492.

622 Desta, Z., Kreutz, Y., Nguyen, A. T., Li, L., Skaar, T., Kamdem, L. K., et al. (2011). Plasma
623 letrozole concentrations in postmenopausal women with breast cancer are associated
624 with CYP2A6 genetic variants, body mass index, and age. *Clin. Pharmacol. Ther.* 90,
625 693–700. doi:10.1038/clpt.2011.174.

626 Din, O. S., Dodwell, D., Wakefield, R. J., and Coleman, R. E. (2010). Aromatase inhibitor-
627 induced arthralgia in early breast cancer: what do we know and how can we find out
628 more? *Breast Cancer Res. Treat.* 120, 525–538. doi:10.1007/s10549-010-0757-7.

629 Evrard, H. C., and Balthazart, J. (2004a). Aromatization of androgens into estrogens reduces
630 response latency to a noxious thermal stimulus in male quail. *Hormones and Behavior*
631 45, 181–189. doi:10.1016/j.yhbeh.2003.09.014.

632 Evrard, H. C., and Balthazart, J. (2004b). Rapid Regulation of Pain by Estrogens Synthesized
633 in Spinal Dorsal Horn Neurons. *J. Neurosci.* 24, 7225–7229.
634 doi:10.1523/JNEUROSCI.1638-04.2004.

635 Fillingim, R. B., and Ness, T. J. (2000). Sex-related hormonal influences on pain and
636 analgesic responses. *Neuroscience & Biobehavioral Reviews* 24, 485–501.
637 doi:10.1016/S0149-7634(00)00017-8.

638 Fusi, C., Materazzi, S., Benemei, S., Coppi, E., Trevisan, G., Marone, I. M., et al. (2014).
639 Steroidal and non-steroidal third-generation aromatase inhibitors induce pain-like
640 symptoms via TRPA1. *Nat Commun* 5, 5736. doi:10.1038/ncomms6736.

641 Gaillard, S., and Stearns, V. (2011). Aromatase inhibitor-associated bone and musculoskeletal
642 effects: new evidence defining etiology and strategies for management. *Breast Cancer*
643 *Res.* 13, 205. doi:10.1186/bcr2818.

644 Gasser, J. A., Green, J. R., Shen, V., Ingold, P., Rebmann, A., Bhatnagar, A. S., et al. (2006).
645 A single intravenous administration of zoledronic acid prevents the bone loss and
646 mechanical compromise induced by aromatase inhibition in rats. *Bone* 39, 787–795.
647 doi:10.1016/j.bone.2006.04.035.

648 Gérard, C., Gallez, A., Dubois, C., Drion, P., Delahaut, P., Quertemont, E., et al. (2017).
649 Accurate Control of 17β-Estradiol Long-Term Release Increases Reliability and
650 Reproducibility of Preclinical Animal Studies. *J Mammary Gland Biol Neoplasia* 22,
651 1–11. doi:10.1007/s10911-016-9368-1.

652 Ghorbanpoor, S., Garcia-Segura, L. M., Haeri-Rohani, A., Khodagholi, F., and Jorjani, M.
653 (2014). Aromatase inhibition exacerbates pain and reactive gliosis in the dorsal horn

654 of the spinal cord of female rats caused by spinothalamic tract injury. *Endocrinology*
655 155, 4341–4355. doi:10.1210/en.2014-1158.

656 Giorgi, S., Nikolaeva-Koleva, M., Alarcón-Alarcón, D., Butrón, L., and González-Rodríguez,
657 S. (2019). Is TRPA1 Burning Down TRPV1 as Druggable Target for the Treatment of
658 Chronic Pain? *Int J Mol Sci* 20. doi:10.3390/ijms20122906.

659 Goss, P. E., Ingle, J. N., Martino, S., Robert, N. J., Muss, H. B., Piccart, M. J., et al. (2005).
660 Randomized trial of letrozole following tamoxifen as extended adjuvant therapy in
661 receptor-positive breast cancer: updated findings from NCIC CTG MA.17. *J. Natl.*
662 *Cancer Inst.* 97, 1262–1271. doi:10.1093/jnci/dji250.

663 Goss, P. E., Ingle, J. N., Pritchard, K. I., Robert, N. J., Muss, H., Gralow, J., et al. (2016).
664 Extending Aromatase-Inhibitor Adjuvant Therapy to 10 Years. *New England Journal*
665 *of Medicine*. doi:10.1056/NEJMoa1604700.

666 Goss, P. E., Qi, S., Cheung, A. M., Hu, H., Mendes, M., and Pritzker, K. P. H. (2004). Effects
667 of the steroidal aromatase inhibitor exemestane and the nonsteroidal aromatase
668 inhibitor letrozole on bone and lipid metabolism in ovariectomized rats. *Clin. Cancer*
669 *Res.* 10, 5717–5723. doi:10.1158/1078-0432.CCR-04-0438.

670 Goss, P. E., Qi, S., Hu, H., and Cheung, A. M. (2007). The effects of atamestane and
671 toremifene alone and in combination compared with letrozole on bone, serum lipids
672 and the uterus in an ovariectomized rat model. *Breast Cancer Res. Treat.* 103, 293–
673 302. doi:10.1007/s10549-006-9381-y.

674 Henry, N. L., Azzouz, F., Desta, Z., Li, L., Nguyen, A. T., Lemler, S., et al. (2012). Predictors
675 of aromatase inhibitor discontinuation as a result of treatment-emergent symptoms in
676 early-stage breast cancer. *J. Clin. Oncol.* 30, 936–942.
677 doi:10.1200/JCO.2011.38.0261.

678 Henry, N. L., Giles, J. T., Ang, D., Mohan, M., Dadabhoy, D., Robarge, J., et al. (2008).
679 Prospective characterization of musculoskeletal symptoms in early stage breast cancer
680 patients treated with aromatase inhibitors. *Breast Cancer Res. Treat.* 111, 365–372.
681 doi:10.1007/s10549-007-9774-6.

682 Henry, N. L., Unger, J. M., Schott, A. F., Fehrenbacher, L., Flynn, P. J., Prow, D. M., et al.
683 (2018). Randomized, Multicenter, Placebo-Controlled Clinical Trial of Duloxetine
684 Versus Placebo for Aromatase Inhibitor-Associated Arthralgias in Early-Stage Breast
685 Cancer: SWOG S1202. *J. Clin. Oncol.* 36, 326–332. doi:10.1200/JCO.2017.74.6651.

686 Jakesz, R., Jonat, W., Gnant, M., Mittlboeck, M., Greil, R., Tausch, C., et al. (2005).
687 Switching of postmenopausal women with endocrine-responsive early breast cancer to
688 anastrozole after 2 years' adjuvant tamoxifen: combined results of ABCSG trial 8 and
689 ARNO 95 trial. *Lancet* 366, 455–462. doi:10.1016/S0140-6736(05)67059-6.

690 Kafali, H., Iriadam, M., Ozardalı, I., and Demir, N. (2004). Letrozole-induced polycystic
691 ovaries in the rat: a new model for cystic ovarian disease. *Archives of Medical*
692 *Research* 35, 103–108. doi:10.1016/j.arcmed.2003.10.005.

693 Kilkenny, C., Browne, W. J., Cuthill, I. C., Emerson, M., and Altman, D. G. (2010).
694 Improving bioscience research reporting: The ARRIVE guidelines for reporting

695 animal research. *J Pharmacol Pharmacother* 1, 94–99. doi:10.4103/0976-
696 500X.72351.

697 Kim, J.-S., Kroin, J. S., Li, X., An, H. S., Buvanendran, A., Yan, D., et al. (2011). The rat
698 intervertebral disk degeneration pain model: relationships between biological and
699 structural alterations and pain. *Arthritis Res Ther* 13, R165. doi:10.1186/ar3485.

700 Kistner, K., Siklosi, N., Babes, A., Khalil, M., Selescu, T., Zimmermann, K., et al. (2016).
701 Systemic desensitization through TRPA1 channels by capsazepine and mustard oil - a
702 novel strategy against inflammation and pain. *Sci Rep* 6. doi:10.1038/srep28621.

703 Koebele, S. V., and Bimonte-Nelson, H. A. (2016). Modeling menopause: The utility of
704 rodents in translational behavioral endocrinology research. *Maturitas* 87, 5–17.
705 doi:10.1016/j.maturitas.2016.01.015.

706 Kokras, N., Pastromas, N., Papasava, D., de Bournonville, C., Cornil, C. A., and Dalla, C.
707 (2018). Sex differences in behavioral and neurochemical effects of gonadectomy and
708 aromatase inhibition in rats. *Psychoneuroendocrinology* 87, 93–107.
709 doi:10.1016/j.psyneuen.2017.10.007.

710 Kumru, S., Yildiz, A. A., Yilmaz, B., Sandal, S., and Gurates, B. (2007). Effects of aromatase
711 inhibitors letrozole and anastrazole on bone metabolism and steroid hormone levels in
712 intact female rats. *Gynecol. Endocrinol.* 23, 556–561.
713 doi:10.1080/09513590701557119.

714 Liu, X. D., Xie, L., Zhong, Y., and Li, C. X. (2000). Gender difference in letrozole
715 pharmacokinetics in rats. *Acta Pharmacol. Sin.* 21, 680–684.

716 Mamounas, E. P., Bandos, H., Lembersky, B. C., Jeong, J.-H., Geyer, C. E., Rastogi, P., et al.
717 (2019). Use of letrozole after aromatase inhibitor-based therapy in postmenopausal
718 breast cancer (NRG Oncology/NSABP B-42): a randomised, double-blind, placebo-
719 controlled, phase 3 trial. *The Lancet Oncology* 20, 88–99. doi:10.1016/S1470-
720 2045(18)30621-1.

721 Meng, F.-T., Ni, R.-J., Zhang, Z., Zhao, J., Liu, Y.-J., and Zhou, J.-N. (2011). Inhibition of
722 oestrogen biosynthesis induces mild anxiety in C57BL/6J ovariectomized female
723 mice. *Neurosci Bull* 27, 241–250. doi:10.1007/s12264-011-1014-8.

724 Miller, K. D., Nogueira, L., Mariotto, A. B., Rowland, J. H., Yabroff, K. R., Alfano, C. M., et
725 al. (2019). Cancer treatment and survivorship statistics, 2019. *CA Cancer J Clin* 69,
726 363–385. doi:10.3322/caac.21565.

727 Miller, K. D., Siegel, R. L., Lin, C. C., Mariotto, A. B., Kramer, J. L., Rowland, J. H., et al.
728 (2016). Cancer treatment and survivorship statistics, 2016. *CA Cancer J Clin* 66, 271–
729 289. doi:10.3322/caac.21349.

730 Mohamed, I., and Yeh, J. K. (2009). Alfacalcidol prevents aromatase inhibitor (Letrozole)-
731 induced bone mineral loss in young growing female rats. *J. Endocrinol.* 202, 317–325.
732 doi:10.1677/JOE-08-0532.

Moradi-Azani, M., Ahmadiani, A., and Amini, H. (2011). Increase in formalin-induced tonic pain by 5alpha-reductase and aromatase inhibition in female rats. *Pharmacology Biochemistry and Behavior* 98, 62–66. doi:10.1016/j.pbb.2010.12.016.

Mosquera, L., Shepherd, L., Torrado, A. I., Torres-Diaz, Y. M., Miranda, J. D., and Segarra, A. C. (2015). Comparison of Two Methods of Estradiol Replacement: their Physiological and Behavioral Outcomes. *J Vet Sci Technol* 6, 276. doi:10.4172/2157-7579.1000276.

Nabieva, N., Häberle, L., Brucker, S. Y., Janni, W., Volz, B., Loehberg, C. R., et al. (2019). Preexisting musculoskeletal burden and its development under letrozole treatment in early breast cancer patients. *Int. J. Cancer* 145, 2114–2121. doi:10.1002/ijc.32294.

Niravath, P. (2013). Aromatase inhibitor-induced arthralgia: a review. *Ann. Oncol.* 24, 1443–1449. doi:10.1093/annonc/mdt037.

Ortega, I., Sokalska, A., Villanueva, J. A., Cress, A. B., Wong, D. H., Stener-Victorin, E., et al. (2013). Letrozole increases ovarian growth and Cyp17a1 gene expression in the rat ovary. *Fertil. Steril.* 99, 889–896. doi:10.1016/j.fertnstert.2012.11.006.

Partridge, A. H., LaFountain, A., Mayer, E., Taylor, B. S., Winer, E., and Asnis-Alibozek, A. (2008). Adherence to initial adjuvant anastrozole therapy among women with early-stage breast cancer. *J. Clin. Oncol.* 26, 556–562. doi:10.1200/JCO.2007.11.5451.

Perez, E. A., Josse, R. G., Pritchard, K. I., Ingle, J. N., Martino, S., Findlay, B. P., et al. (2006). Effect of letrozole versus placebo on bone mineral density in women with primary breast cancer completing 5 or more years of adjuvant tamoxifen: a companion study to NCIC CTG MA.17. *J. Clin. Oncol.* 24, 3629–3635. doi:10.1200/JCO.2005.05.4882.

Pfister, C. U., Martoni, A., Zamagni, C., Lelli, G., De Braud, F., Souppart, C., et al. (2001). Effect of age and single versus multiple dose pharmacokinetics of letrozole (Femara) in breast cancer patients. *Biopharm Drug Dispos* 22, 191–197. doi:10.1002/bdd.273.

Pineda-Moncusí, M., Servitja, S., Casamayor, G., Cos, M. L., Rial, A., Rodriguez-Morera, J., et al. (2018). Bone health evaluation one year after aromatase inhibitors completion. *Bone* 117, 54–59. doi:10.1016/j.bone.2018.09.010.

Raisinghani, M., Zhong, L., Jeffry, J. A., Bishnoi, M., Pabbidi, R. M., Pimentel, F., et al. (2011). Activation characteristics of transient receptor potential ankyrin 1 and its role in nociception. *Am J Physiol Cell Physiol* 301, C587–C600. doi:10.1152/ajpcell.00465.2010.

Ratka, A., and Simpkins, J. W. (1991). Effects of estradiol and progesterone on the sensitivity to pain and on morphine-induced antinociception in female rats. *Horm Behav* 25, 217–228. doi:10.1016/0018-506x(91)90052-j.

Renczés, E., Borbélyová, V., Steinhardt, M., Höpfner, T., Stehle, T., Ostatníková, D., et al. (2020). The Role of Estrogen in Anxiety-Like Behavior and Memory of Middle-Aged Female Rats. *Front Endocrinol (Lausanne)* 11, 570560. doi:10.3389/fendo.2020.570560.

773 Robarge, J. D., Duarte, D. B., Shariati, B., Wang, R., Flockhart, D. A., and Vasko, M. R.
774 (2016). Aromatase inhibitors augment nociceptive behaviors in rats and enhance the
775 excitability of sensory neurons. *Exp. Neurol.* 281, 53–65.
776 doi:10.1016/j.expneurol.2016.04.006.

777 Roche, L., Pinguet, J., Herviou, P., Libert, F., Chenaf, C., Eschalier, A., et al. (2016). Fully
778 automated semi-quantitative toxicological screening in three biological matrices using
779 turbulent flow chromatography/high resolution mass spectrometry. *Clinica Chimica*
780 *Acta* 455, 46–54. doi:10.1016/j.cca.2016.01.017.

781 Rosales Rocabado, J. M., Kaku, M., Nozaki, K., Ida, T., Kitami, M., Aoyagi, Y., et al. (2018).
782 A multi-factorial analysis of bone morphology and fracture strength of rat femur in
783 response to ovariectomy. *J Orthop Surg Res* 13, 318. doi:10.1186/s13018-018-1018-4.

784 Sengupta, P. (2013). The Laboratory Rat: Relating Its Age With Human's. *International*
785 *Journal of Preventive Medicine* 4, 624–630.

786 Siegel, R., DeSantis, C., Virgo, K., Stein, K., Mariotto, A., Smith, T., et al. (2012). Cancer
787 treatment and survivorship statistics, 2012. *CA: A Cancer Journal for Clinicians* 62,
788 220–241. doi:10.3322/caac.21149.

789 Tenti, S., Correale, P., Cheleschi, S., Fioravanti, A., and Pirtoli, L. (2020). Aromatase
790 Inhibitors-Induced Musculoskeletal Disorders: Current Knowledge on Clinical and
791 Molecular Aspects. *Int J Mol Sci* 21. doi:10.3390/ijms21165625.

792 Tsao, C. M., Ho, C. M., Tsai, S. K., and Lee, T. Y. (1999). Effects of estrogen on autotomy in
793 normal and ovariectomized rats. *Pharmacology* 59, 142–148. doi:10.1159/000028314.

794 Verbeke, G., and Molenberghs, G. (2009). *Linear mixed models for longitudinal data*. New
795 York: Springer.

796 Vincent, K., and Tracey, I. (2008). Hormones and their Interaction with the Pain Experience.
797 *Reviews in Pain* 2, 20–24. doi:10.1177/204946370800200206.

798 Wang, X.-L., Cui, L.-W., Liu, Z., Gao, Y.-M., Wang, S., Li, H., et al. (2019). Effects of
799 TRPA1 activation and inhibition on TRPA1 and CGRP expression in dorsal root
800 ganglion neurons. *Neural Regen Res* 14, 140–148. doi:10.4103/1673-5374.243719.

801
802

803 **Figure 1: Conduct of experiments**

804 Experiments were repeated 3 times and the results were pooled for the final analysis. At day
805 0, four groups of animals were defined: sham animals with a vehicle pellet (SHAM+VEH
806 n=13), ovariectomized animals with a vehicle pellet (OVX+VEH; n=14), and ovariectomized
807 animals with a pellet of LTZ 200 µg/day (OVX+PLT 200; n=14) or LTZ 400 µg/day
808 (OVX+PLT 400; n=15)

809

810 **Figure 2: Selection of AI-treated rats assessing LTZ plasma level after 73 days**

811 Animals were OVX or not (Sham+VEH; n=13) and then treated with vehicle (OVX+VEH;
812 n=14) or pellets of LTZ 200 µg/day (OVX+PLT 200; n=14) or 400 µg/day (OVX+PLT 400;
813 n=15) (**A**). Rats with plasma level higher than 90 ng/mL (**B**) were then included among the
814 OVX+HIGH LTZ (n=11). Rats with plasma level less than 90 ng/mL were then included
815 among the OVX+LOW LTZ (n=18). Data are presented as the mean ± SEM. *** $p<0.001$.

816

817 **Figure 3: Increase in OVX-rat weight during experiments**

818 Data are presented as the mean ± SEM (SHAM+VEH n=14, OVX+VEH n=14, OVX+LOW
819 LTZ n=18 and OVX+HIGH LTZ n=11). ** $p<0.01$ and *** $p<0.001$ vs (OVX+VEH,
820 OVX+LOW LTZ and OVX+HIGH LTZ).

821

822 **Figure 4: No alteration in locomotion in AI-treated rats**

823 Motor coordination was evaluated weekly using the rotarod test (**A**) for up to 73 days.
824 Locomotion (distance traveled (cm) and velocity (cm/s)) and experimental anxiety (inner zone
825 duration (s)) were assessed using the open field test at day 49 (**B**). For the rotarod test, data
826 are presented as the mean ± SEM compared to baseline value and the area under the curve
827 (AUC) (**A**: SHAM+VEH n=7, OVX+VEH n=9, OVX+LOW LTZ n=10, and OVX+HIGH

828 LTZ n=8). For the open field test, data are presented as the mean ± SEM (**B**: SHAM+VEH
829 n=14, OVX+VEH n=14, OVX+LOW LTZ n=18 and OVX+HIGH LTZ n=11). Each group
830 was compared to OVX+VEH.
831
832 **Figure 5: Occurrence of long-term nociceptive disorders (ankle pressure test) but not**
833 **myalgia in AI-treated rats**
834 Mechanical thresholds of nociceptive disorders were assessed using ankle pressure (**A**) and
835 Smalgo (**B**) tests, respectively. Data are presented as the mean ± SEM compared to baseline
836 value and area under the curve (AUC) (**A**: SHAM+VEH n=12, OVX+VEH n=12,
837 OVX+LOW LTZ n=18, and OVX+HIGH LTZ n=11) and (**B**: SHAM+VEH n=14,
838 OVX+VEH n=14, OVX+LOW LTZ n=18, and OVX+HIGH LTZ n=11). * $p<0.05$, **
839 $p<0.01$. Each group was compared to OVX+VEH.
840
841 **Figure 6: No significant modification in TRPA1 expression in AI-treated rats**
842 In summary, rats were sacrificed and protein expression in DRG was evaluated by western-
843 blotting. Data are presented as the mean of protein expression ± SEM (OVX+VEH n=11 and
844 OVX+HIGH LTZ n=9). The OVX+HIGH LTZ group was compared to OVX+VEH (p=0.20).
845
846

847 **Table 1: Alteration of bone architecture in OVX+LOW LTZ and OVX+HIGH LTZ rats**

848 Bone architectural modifications of the femora were evaluated using micro-computed
849 tomography scans analyses. Results are presented as the mean ± standard deviation for bone
850 volume fraction of the femora (BV/TV), bone volume ratio (BS/TV), trabecular thickness
851 (Tb.Th), trabecular separation (Tb.Sp), trabecular number (Tb.N), trabecular bone pattern
852 factor (Tb.Pf), degree of anisotropy (DA), and structure model index (SMI) (SHAM+VEH
853 n=4, OVX+VEH n=5, OVX+LOW LTZ n=5, and OVX+HIGH LTZ n=6). # $p<0.05$ and ##
854 $p<0.01$ vs SHAM+VEH

855

	SHAM+VEH	OVX+VEH	OVX+LOW LTZ	OVX+HIGH LTZ
BV/TV (%)	22.0 ± 8.4	4.1 ± 1.7 *	3.2 ± 1.8 **	3.4 ± 2.1 **
BS/TV (mm^{-1})	6.4 ± 1.7	1.5 ± 0.5 *	1.2 ± 0.6 **	1.3 ± 0.7 **
Tb.Th (mm)	0.126 ± 0.013	0.112 ± 0.011	0.112 ± 0.007 *	0.108 ± 0.012 **
Tb.Sp (mm)	0.42 ± 0.13	1.55 ± 0.17 *	1.53 ± 0.12 *	1.65 ± 0.23 **
Tb.N (mm^{-1})	1.70 ± 0.51	0.36 ± 0.13 *	0.28 ± 0.16 **	0.30 ± 0.18 **
Tb.Pf	3.8 ± 3.7	12.2± 1.9 *	14.2 ± 2.9 **	14.7 ± 5.4 **
DA	1.7 ± 0.1	1.7 ± 0.2	1.8 ± 0.6	1.7 ± 0.5
SMI	1.74 ± 0.33	2.48 ± 0.13 *	2.58 ± 0.19 **	2.56 ± 0.26 *

856
857

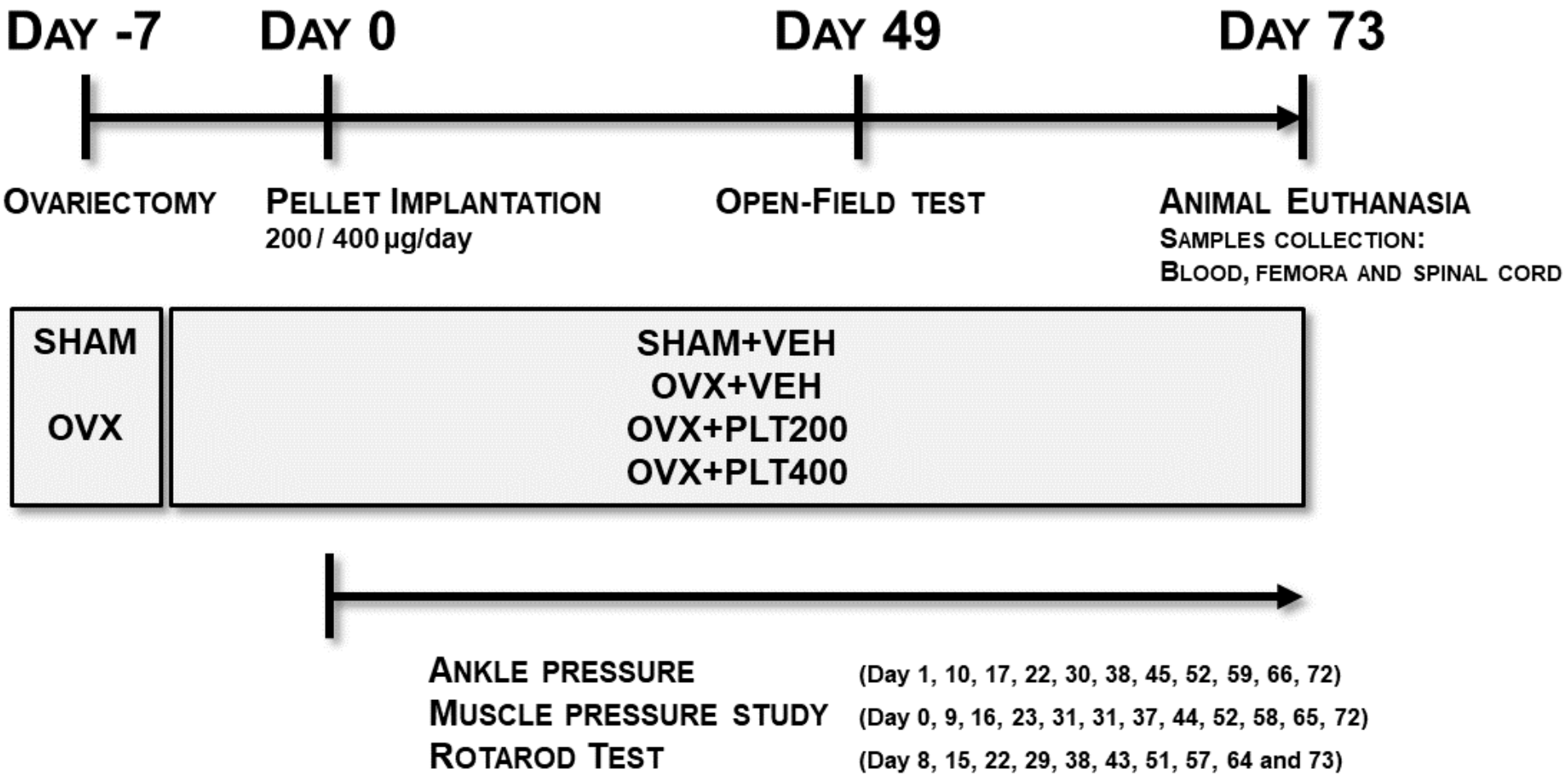
DAY -7
DAY 0
DAY 49
DAY 73
OVARIECTOMY
PELLET IMPLANTATION
200 / 400 µg/day
OPEN-FIELD TEST
ANIMAL EUTHANASIA
SAMPLES COLLECTION:
BLOOD, FEMORA AND SPINAL CORD
SHAM
OVX
SHAM+VEH
OVX+VEH
OVX+PLT200
OVX+PLT400
ANKLE PRESSURE (Day 1, 10, 17, 22, 30, 38, 45, 52, 59, 66, 72)
MUSCLE PRESSURE STUDY (Day 0, 9, 16, 23, 31, 31, 37, 44, 52, 58, 65, 72)
ROTAROD TEST (Day 8, 15, 22, 29, 38, 43, 51, 57, 64 and 73)

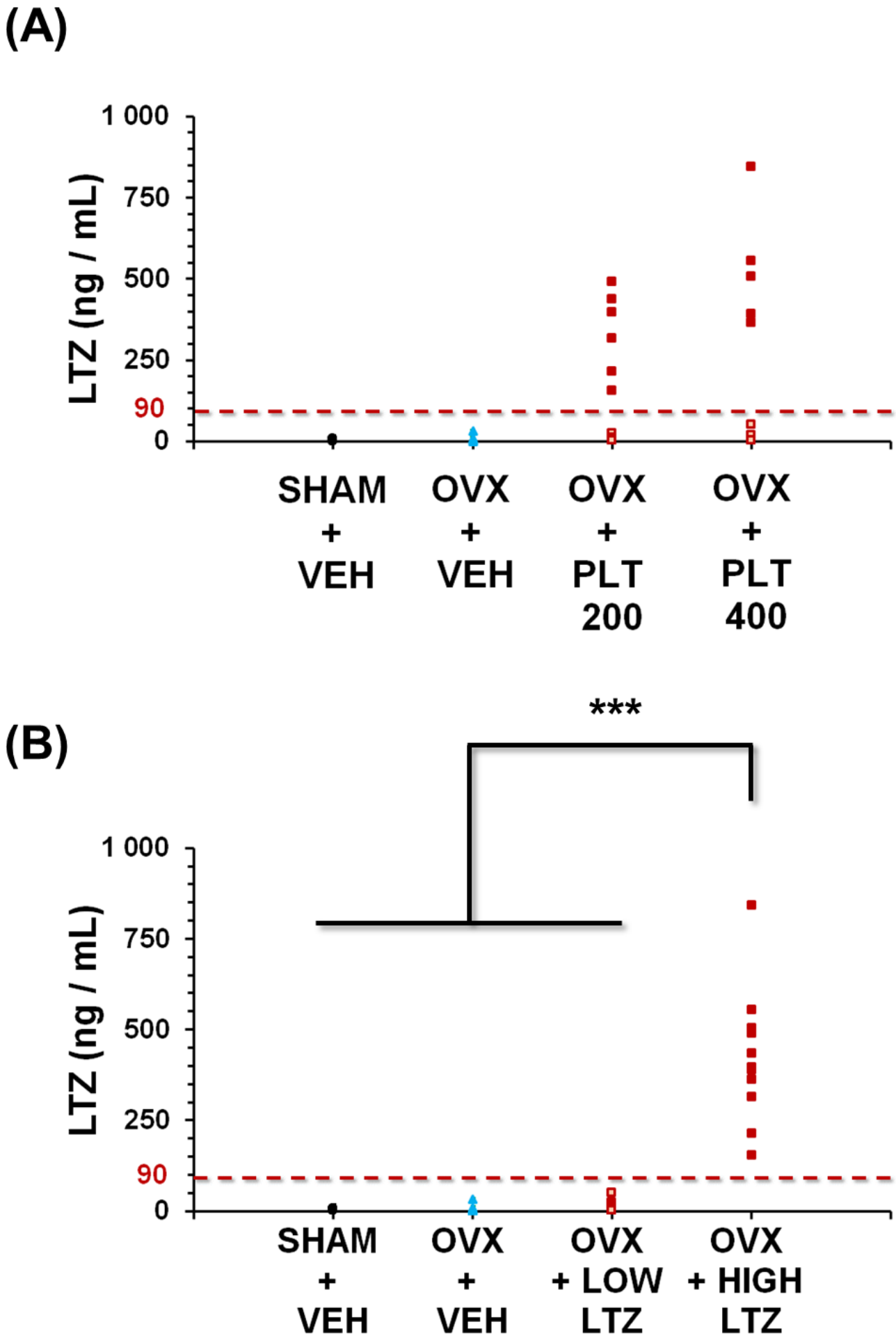
(A)
LTZ (ng / mL)
1 000
750
500
250
90
0
SHAM + VEH
OVX + VEH
OVX + PLT 200
OVX + PLT 400
(B)
***
LTZ (ng / mL)
1 000
750
500
250
90
0
SHAM + VEH
OVX + VEH
OVX + LOW LTZ
OVX + HIGH LTZ

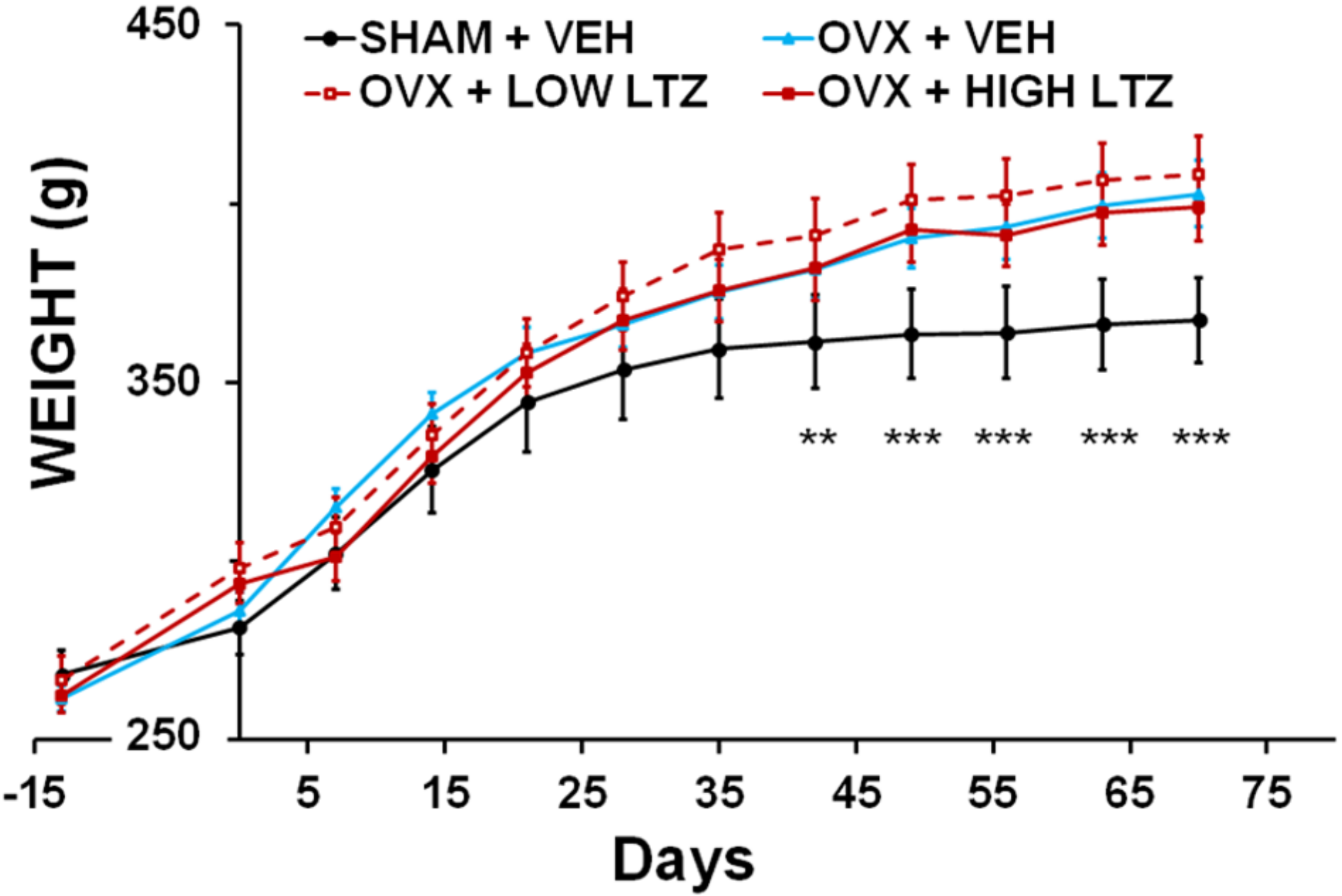
SHAM + VEH
OVX + VEH
OVX + LOW LTZ
OVX + HIGH LTZ
WEIGHT (g)
450
350
250
**
***
***
***
***
-15
5
15
25
35
45
55
65
75
Days

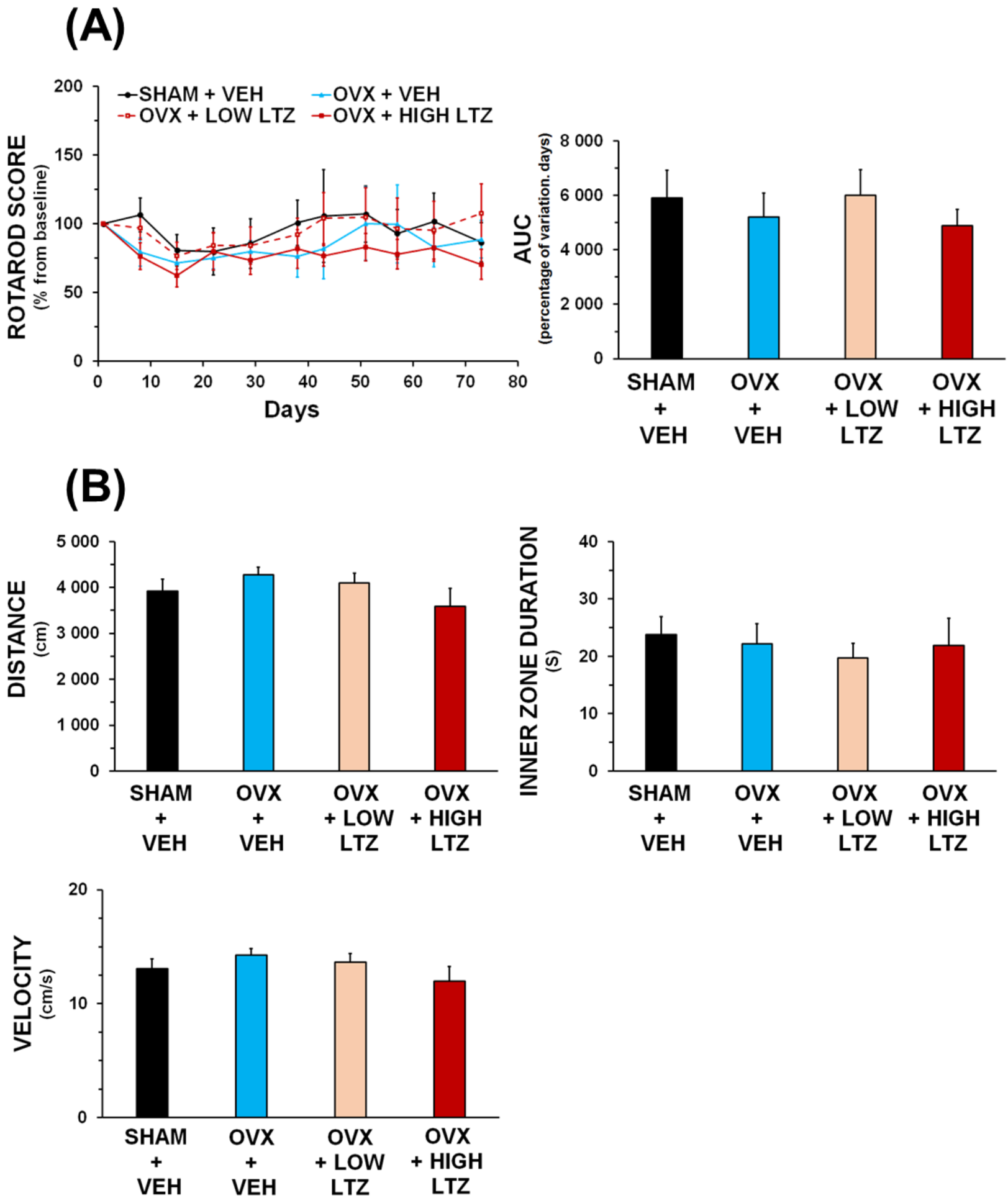
(A)
SHAM + VEH
OVX + VEH
OVX + LOW LTZ
OVX + HIGH LTZ
ROTAROD SCORE
(% from baseline)
Days
AUC
(percentage of variation. days)
SHAM + VEH
OVX + VEH
OVX + LOW LTZ
OVX + HIGH LTZ
(B)
DISTANCE
(cm)
INNER ZONE DURATION
(s)
VELOCITY
(cm/s)

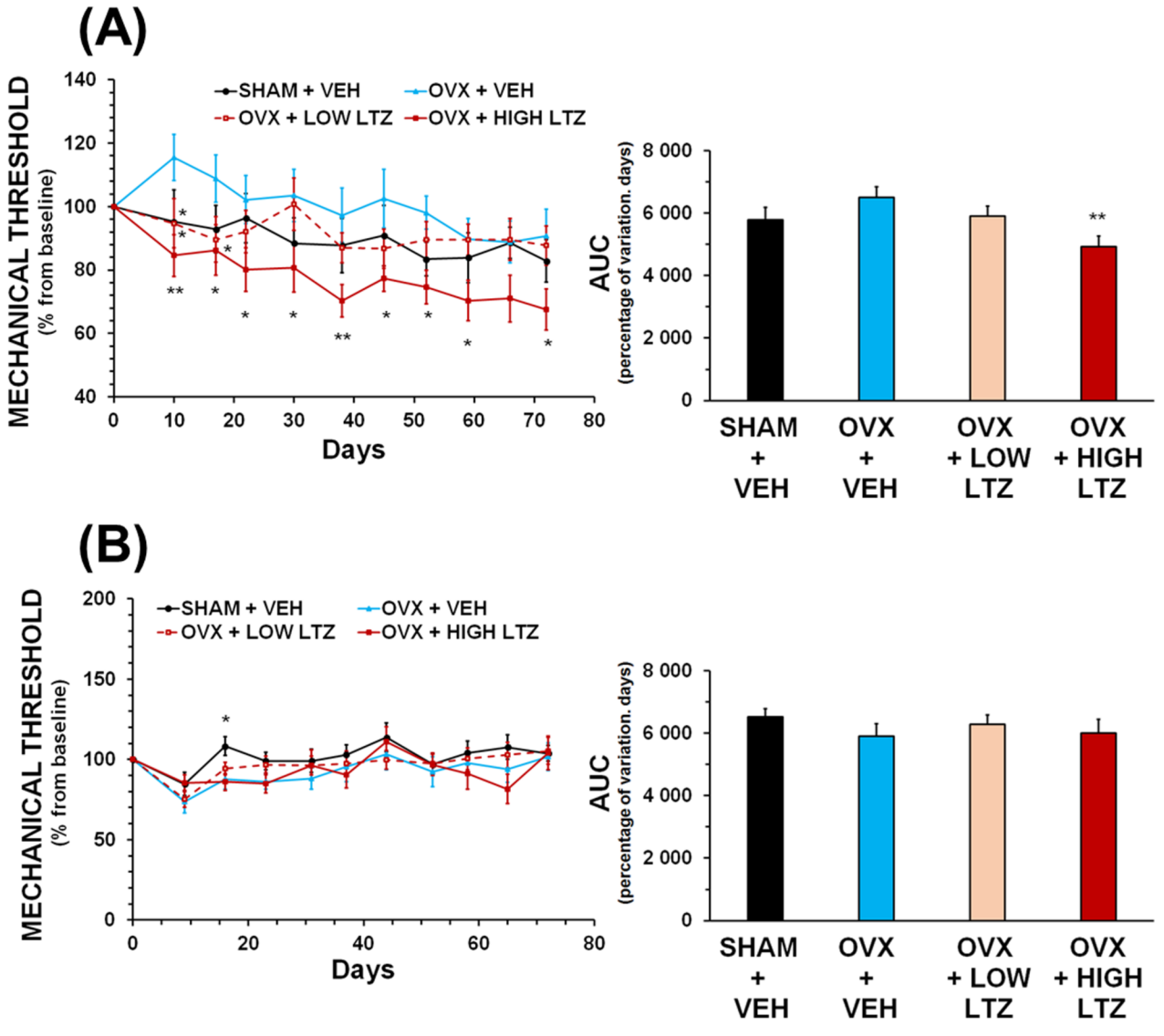
(A)
MECHANICAL THRESHOLD
(% from baseline)
SHAM + VEH
OVX + VEH
OVX + LOW LTZ
OVX + HIGH LTZ
Days
AUC
(percentage of variation. days)
SHAM + VEH
OVX + VEH
OVX + LOW LTZ
OVX + HIGH LTZ
(B)
MECHANICAL THRESHOLD
(% from baseline)
SHAM + VEH
OVX + VEH
OVX + LOW LTZ
OVX + HIGH LTZ
Days
AUC
(percentage of variation. days)
SHAM + VEH
OVX + VEH
OVX + LOW LTZ
OVX + HIGH LTZ

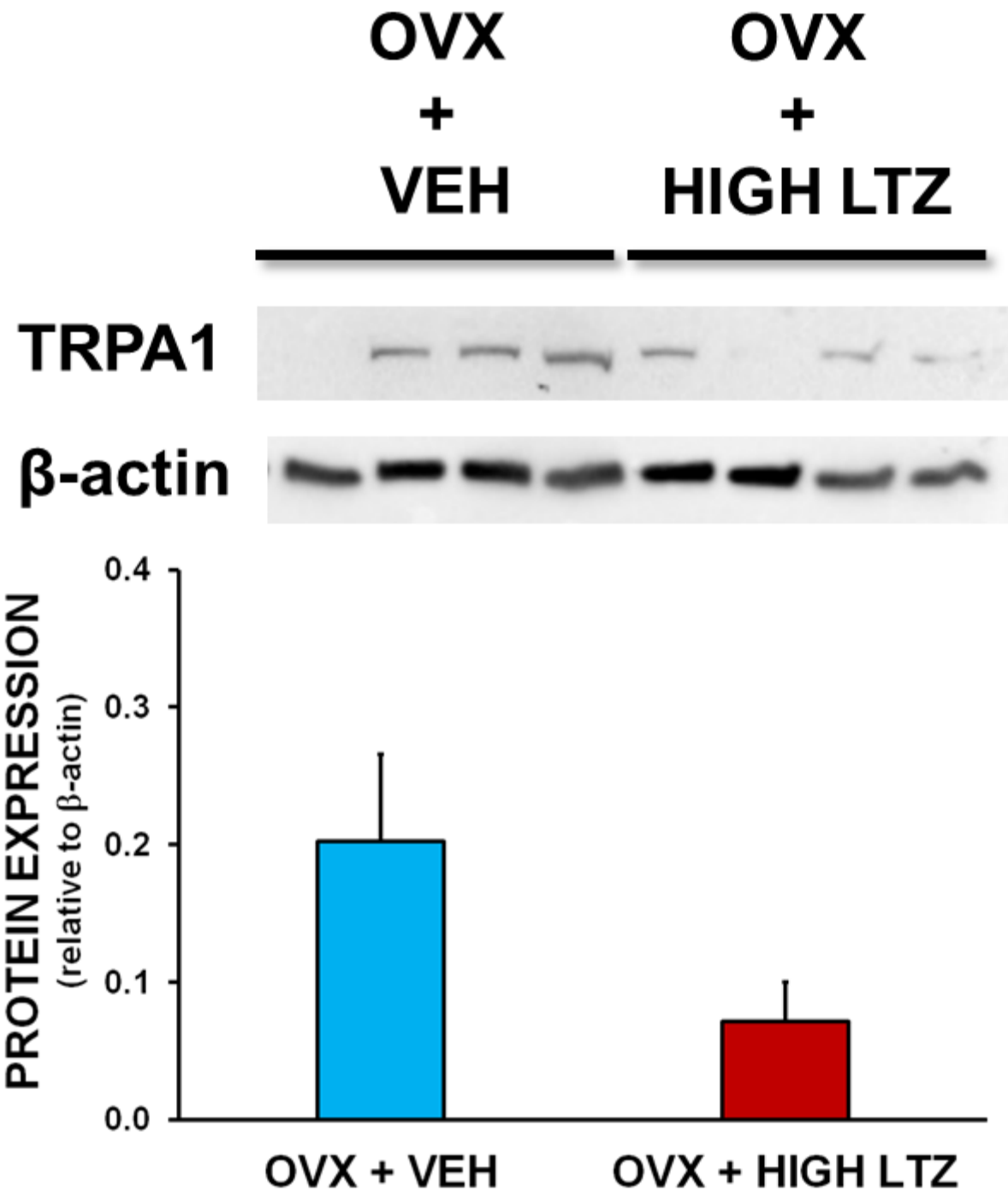
OVX
+
VEH
OVX
+
HIGH LTZ
TRPA1
β-actin
PROTEIN EXPRESSION
(relative to β-actin)
0.4
0.3
0.2
0.1
0.0
OVX + VEH
OVX + HIGH LTZ